Innervation of Tissue-Engineered Corneal Implants in a Porcine Model: A 1-Year In Vivo Confocal Microscopy Study

Neil S. Lagali,[1] *May Griffith,*[1,2] *Naoshi Shinozaki,*[3] *Per Fagerholm,*[4] *and Rejean Munger*[1]

Purpose. To examine the pattern of nerve regeneration within tissue-engineered corneal substitutes grafted into host porcine corneas over a 1-year postoperative period.

Methods. Biodegradable corneal substitutes from cross-linked collagen were implanted into the left eyes of 12 pigs by deep lamellar keratoplasty. Regeneration of severed nerves into the central implant region was investigated with in vivo confocal microscopy. Both implant-recipient and control (right) eyes were examined before surgery and 2, 6, 10, and 12 months after surgery, to quantify the number, density, diameter, and branching of nerve fiber bundles at various corneal depths. Transmission electron microscopy was used to confirm the presence of nerve bundles.

Results. Two months after surgery, corneal nerve ingrowth was observed within the deep anterior stroma, with a number and density of regenerated nerves significantly higher than in nonsurgical control eyes ($P < 0.01$). Nerves within the superficial anterior stroma regenerated by 6 to 10 months after surgery, and the first subbasal epithelial nerves were seen 10 months after surgery. After 1 year, subbasal nerve density recovered to preoperative levels. Nerve fibers in the deep anterior stroma remained significantly thinner relative to control eyes after 1 year ($P < 0.001$), where both superficial anterior and subbasal nerve diameter did not change relative to control eyes.

Conclusions. The pattern of reinnervation within tissue-engineered corneal substitutes has been quantified in vivo. Innervation proceeded rapidly in the deep anterior stroma, followed by repopulation of more superficial regions. One year after surgery, nerve density within the tissue-engineered cornea increased or remained unchanged relative to controls in all corneal regions examined. (*Invest Ophthalmol Vis Sci.* 2007; 48:3537–3544) DOI:10.1167/iovs.06-1483

Cornea-related vision loss affects millions worldwide,[1] and the only currently accepted medical treatment is transplantation of human donor corneas. A worldwide shortage of acceptable donor corneas has prompted research into corneal substitutes suitable for implantation. Recently, we developed a simple corneal substitute that is based on cross-linked collagen that was transplanted into pigs by deep lamellar keratoplasty, resulting in regeneration of corneal epithelium, stroma, and nerves over 6 months.[2,3] Although nerve regeneration has been observed, the pattern and nature of the reinnervation has not been described, and, restoration of normal corneal sensitivity, wound repair, long-term integrity, and functional viability of the cornea are critically dependent on the degree and nature of reinnervation.[4]

Quantitative studies of innervation within the living cornea have been undertaken by several groups in recent years.[5–7] The adoption of clinical in vivo confocal microscopy has elucidated the pattern of normal innervation within the human cornea,[5,7] as well as abnormal nerve patterns indicative of disease[8–10] or surgical trauma—particularly from photorefractive procedures.[11–14] Although the body of quantitative nerve data from human subjects continues to grow, there is little information about the normal pattern of innervation within the porcine cornea—a model closely resembling the human cornea and widely used in experimental corneal surgery. Moreover, there is only sparse information available on reinnervation of donor corneal buttons after transplantation,[15–18] and no quantitative data on reinnervation of any known tissue-engineered corneal substitute to date. The objective of the present study, therefore, was to report on the pattern of nerve regrowth and in-growth into a tissue-engineered corneal substitute over a 12-month postoperative period using quantitative in vivo confocal microscopy. Transmission electron microscopy was used to confirm the presence of nerves within the fabricated corneal substitute.

Methods

Tissue-Engineered Cornea Construction

In contrast to earlier tissue-engineered corneas based on a collagen-copolymer system,[2] a simpler cross-linked collagen system was used in this study, the details of which are reported elsewhere.[3] Two tissue-engineered cornea formulations were used in this study that differed with respect to the addition of chondroitin sulfate to the collagen in one formulation. Chondroitin sulfate is a glycosaminoglycan that comprises the ground substance in the extracellular matrix of the cornea, with a reported effect in promoting nerve growth.[19] The chemical composition of the tissue-engineered cornea formulations was 10% (wt/wt) porcine collagen, cross-linked with 1-ethyl-3-(3-dimethylaminopropyl)carbodiimide (EDC) and its co-reagent *N*-hydroxysuccinimide (NHS; $n = 8$ pigs); and 10% (wt/wt) porcine collagen with 1% (wt/wt) chondroitin sulfate, also cross-linked with EDC and NHS ($n = 4$).

Surgical Procedure and Postoperative Treatment

Twelve 6-month-old neutered male Gottingen mini-pigs (Marshall Farms, North Rose, NY) were obtained for the study, with an average weight of 55 kg at surgery. According to animal use guidelines set by the ARVO Statement for the Use of Animals in Ophthalmic and Vision

From the [1]University of Ottawa Eye Institute and the [2]Department of Cellular and Molecular Medicine, University of Ottawa, Ottawa, ON, Canada; the [3]TDC Eye Bank and Cornea Centre, Ichikawa General Hospital, Chiba, Japan; and the [4]Department of Ophthalmology, Linköping University Hospital, Linköping, Sweden.

Supported by Natural Sciences and Engineering Research Council (NSERC) Canada Grant STPGP 246418-01 (MG); a Canadian Institute of Health Research (CHIR) postdoctoral fellowship (NL); and a contribution from CooperVision for pig corneal implantation studies (MG, RM).

Submitted for publication December 14, 2006; revised March 5 and 26 and April 2, 2007; accepted May 14, 2007.

Disclosure: **N.S. Lagali**, None; **M. Griffith**, Cooper Vision (C, F, P); **N. Shinozaki**, None; **P. Fagerholm**, None; **R. Munger**, Cooper Vision (F)

The publication costs of this article were defrayed in part by page charge payment. This article must therefore be marked "*advertisement*" in accordance with 18 U.S.C. §1734 solely to indicate this fact.

Corresponding author: Rejean Munger, University of Ottawa Eye Institute, The Ottawa Hospital–General Campus, 501 Smyth Road, Ottawa, ON K1H 8L6, Canada; rmunger@ohri.ca.

Research and with ethics approval from the University of Ottawa (protocol EI-5), tissue-engineered corneal substitutes (500-μm thick, 6-mm diameter) were implanted into the left eye of each pig by deep lamellar keratoplasty and held in place with overlying sutures (Zirm retention bridge suturing). The right corneas of all animals were left untouched to serve as control samples. The average porcine corneal thickness before surgery was 680 $\pm$ 78 μm (mean $\pm$ SD), as determined by confocal microscopy (depth difference between epithelial and endothelial images). Immediately after implantation, topical antibiotics were administered to the surgical eye, consisting of 2 drops of gatifloxacin 0.3% (anti-infective; Zymar; Allergan, Irvine, CA) and chloramphenicol ointment 1% (Chloromycetin; Pfizer, New York, NY). The eyelid was then closed with gauze and taped. The postoperative medication regimen consisted of 0.02 mg/kg of 0.3 mg/mL buprenorphine hydrochloride (analgesic; Buprenex, Reckitt and Colman, Parsippany, NJ) given during induction, after surgery and the following morning, 0.2 mg/kg of 1.5 mg/mL metacam (anti-inflammatory; Meloxicam, Boehringer Ingelheim, Germany) given after surgery and 0.1 mg/kg once a day for the following week, and 2 drops of gatifloxacin 0.3% into the surgical eye three times daily for the following week. No steroids were given to any of the animals in this study. Sutures were removed 1 month after surgery. To allow recovery of the surgical eye to proceed unimpeded, we performed the first in vivo confocal microscopy examination 2 months after surgery. As set out in the study protocol, the four animals with collagen-chondroitin sulfate tissue-engineered corneas were killed 10 months after surgery, whereas the remaining eight animals were killed at 1 year.

In Vivo Confocal Microscopy

In vivo confocal microscopy was part of a suite of clinical tests performed on the 12 pigs in a broader study,[3] with images taken 2 months before surgery (12 pigs) and after surgery at 2 (6 pigs), 6 (12 pigs), 10 (4 pigs), and 12 (8 pigs) months using confocal microscopy (Confoscan3; Nidek Technologies Srl., Padova, Italy). To perform an in vivo confocal microscopic examination, we first placed a drop of transparent ophthalmic gel (Tear-gel; Novartis, Mississauga, ON, Canada) on the tip of the objective lens (40×, 0.75 NA, water-immersion objective; Achroplan; Carl Zeiss MicroImaging, Inc., Thornwood, NY), which we then brought into contact with the locally anesthetized cornea (proparacaine hydrochloride 0.5%, Alcaine; Alcon, Fort Worth, TX) of a pig under superficial general anesthesia (0%–5% aerrane; Isoflurane; Baxter, Deerfield, IL). To minimize eye motion, animal respiration was halted for 30 seconds during the confocal examination. The focal plane of the microscope was manually scanned through the full corneal thickness and digital confocal images were captured at 10-μm depth increments and stored on a computer. The confocal field was situated in the central corneal region, as determined by the corneal apex (apical position was verified by uniform central illumination of the captured image), and each image presented a field of view of 440 $\times$ 330 μm (width $\times$ height, frame area = 0.1452 mm^2). A single confocal examination consisted of multiple passes through the cornea (varied due to pig motion; typically two to four), to yield a total of 350 images. Furthermore, multiple examinations (up to three) were made of many corneas (the objective was realigned between each examination), to provide the best possible en face view of corneal features, as an examination sometimes yielded off-center images corresponding to an oblique, out-of-focus view. Although efforts were taken to limit corneal motion during examination, slight axial movements often occurred, resulting in discontinuous data. Using the multipass data within an examination, images duplicated or most likely missed in one pass were manually identified and deleted or replaced with continuous image sequences from another pass to yield the best possible full-thickness corneal scan (composite scan). Within this composite scan, adjacent images were separated by 10 μm in depth, and for each image the depth was recorded relative to the most anterior in-focus image of the corneal epithelial surface (depth, 0 μm).

Nerve Fiber Analysis

A total of 112 in vivo confocal microscopy examinations were performed for the study by a single operator over a 14-month period. For each examination, all images with nerves or nerve fiber bundles (referred to collectively as nerves) were identified. For identification purposes, nerves were defined as bright, slender, straight, or branching structures; as substantially uniform in intensity along their length and width, and as having a marked contrast difference from the background intensity level. Each nerve was counted only once within an examination, and nerves crossing more than one depth image were projected onto one image with a depth taken as the mean depth value of the images. The nerve tracing and analysis software NeuronJ was used in combination with ImageJ software to generate standardized quantitative nerve parameters.[20,21] For each image, the brightness and contrast were adjusted manually to confirm the location of the nerves. Each nerve and branch was manually identified and traced along its length with assistance from the edge detection algorithm within NeuronJ. Nerves were also traced manually across their width to yield an average nerve diameter within each image. For each image, the following parameters were noted: corneal depth location, number of nerves present (each branch with a length >50 μm was counted as a separate nerve[13]), length of each nerve, total nerve length, average nerve diameter, and number of nerve branches. These parameters were used to generate several outcome measures. A total of 783 images containing nerves were analyzed, from which 2322 nerves were traced. Nerve parameters were entered into a spreadsheet for analysis. Image data from repeated examinations at the same time point were excluded from further analysis by retaining only data from the single examination with the greatest total nerve length, which eliminated examinations with oblique, out-of-focus images not representative of the true nerve presence. The resultant data consisted of 622 unique images containing 1835 distinct nerves from 79 examinations.

To describe the location of corneal nerves and to ensure a reliable statistical analysis, we defined three corneal zones. Corneal zones based on depth from the outermost surface of the epithelium were adopted, since some reference anatomic features (such as Bowman's layer) were difficult to identify unambiguously, whereas others were delayed in appearance in the tissue-engineered corneas (e.g., subbasal nerve plexus).

Zone 1. Twenty to 50 μm below the epithelial surface, representing the nerves of the subbasal nerve plexus at the basal epithelial and subepithelial regions, immediately anterior and posterior to the level of the epithelial basement membrane and Bowman's layer.

Zone 2. Sixty to 100 μm below the epithelial surface (sequence of five frames below zone 1), representing the most anterior stromal region.

Zone 3. One hundred ten to 150 μm below the epithelial surface (sequence of five frames below zone 2), representing the deep anterior stroma.

Below a depth of 150 μm, nerves were observed too infrequently in control corneas to allow for a meaningful comparison to be made (only 13 images with nerves located deeper than 150 μm were observed among all control examinations). This scarcity of nerves in the mid to deep stroma is consistent with confocal microscopic observations of the normal central cornea in humans.[13] Because the average porcine central corneal thickness was 680 μm, the nerves detected in this study were primarily superficial or anterior (within the top 25%).

The outcome measures used in this study consisted of nerve density, total number of nerves, total number of branches, and average nerve diameter, all compiled within each depth zone. Nerve density within each depth zone (in micrometers per cubic millimeter) was determined by dividing the total nerve length from all images in the zone by the zone volume, a measure used previously by Calvillo et al.[13] to assess postoperative corneal nerve density changes. To permit a graphic depiction of nerve distribution in the cornea over time, nerve density (in micrometers per cubic millimeter) in steps of two consecutive frames was plotted in relation to corneal depth. The nerve

density was determined by dividing the total nerve length within two consecutive image frames by the sample volume (i.e., frame area × total depth of field; each image had a 26-μm depth of field[22] and was separated by 10 μm, to give a 36 μm total depth of field for two images). In addition, to place nerve density reported in this study in perspective with other reported values, nerve density in the thin subbasal nerve layer was also expressed as total nerve length within a single image frame (in micrometers per square millimeter). Stromal nerves, not confined to a thin layer, had a density dependent on the image depth of field, and so average nerve density in a stromal image frame (in micrometers per cubic millimeter) was used for purposes of comparison.

Transmission Electron Microscopy

After death, both surgical and nonsurgical corneas were processed for routine histopathologic examination after hematoxylin-eosin (H&E) staining. For transmission electron microscopy, the histopathology sections were treated in conventional fixative, stain, and potting resin (Karnovsky's fixative, OsO_4, uranyl acetate, and epoxy). The sections were viewed with a transmission electron microscope (JEM-1010; JEOL, Tokyo, Japan).

Statistical Analysis

Corneal images were sorted according to eye, time of examination, depth zone, and tissue-engineered cornea material formulation. Initially, two-way analysis-of-variance (ANOVA) was performed with the factors of formulation (with or without chondroitin sulfate) and eye (control or surgical). The ANOVA was repeated for each depth zone at preoperative and 6-month postoperative examinations and for the four measures nerve density, nerve diameter, number of nerves, and nerve branches (24 two-way ANOVA tests). For all tests within this study, a $P < 0.05$ was considered statistically significant. The two-way ANOVA revealed significant parameter differences between control and surgical eyes; however, no significant difference in formulation was found with respect to any nerve parameter, nor was any significant interaction between formulation and eye found. As a result, material-dependent effects were not detectable in this study and corneas from all pigs at a given time were grouped in the subsequent analysis. Normality of nerve parameter data was not satisfied for all comparisons of control and surgical corneas (Kolmogorov-Smirnov test, $P < 0.05$), and data were presented as medians and interquartile ranges (Q25, Q75; 25th and 75th percentiles, respectively). Mann-Whitney rank sum tests were used to determine significant differences between control and surgical corneas at each time point. Comparison of nerve parameters longitudinally was performed by single-factor ANOVA. Where longitudinal data was normally distributed with equal variance, one-way ANOVA was used with data also presented as means and standard deviations, whereas Kruskal-Wallis one-way ANOVA on ranks was used for non-normally distributed data. The Holm-Sidak multiple comparison method was used to isolate the significant differences for normally distributed data, whereas the Dunn method was used for data not normally distributed. All statistics were calculated with commercial software (SigmaPlot ver. 9.0 with SigmaStat integration; Systat Software Inc., Point Richmond, CA).

Results

Nerve densities and the number of nerves observed were tabulated (Tables 1, 2; Fig. 3). Both parameters were highly correlated among control and surgical corneas (Pearson's $r >$ 0.95 for both). In nonsurgical control corneas, the greatest density and number of nerves was observed in zone 1, with slightly lower values in zone 2, and sparse nerve presence in zone 3. After surgery in the tissue-engineered corneas, the greatest density and number of nerves was observed in zone 3, with reduced levels in zone 2, and sparse nerve presence in zone 1. The number and density of zone 1 nerves remained constant over time in control eyes, whereas the surgical corneas' nerves in zone 1 were significantly reduced relative to controls in the 6 months after surgery, recovering to control levels at 10 to 12 months. Within zone 2, the number and density of nerves remained constant with time in control eyes,

Table 1. Nerve Density in Central Cornea*

Depth Zone	Cornea	Preoperative	Months after Surgery				ANOVA *P*†
			2	6	10	12	
1	TE	4.1‡ (2.7, 5.8)	0§ (0, 0)	0§ (0, 0)	0‡§ (0, 1.4)	1.0‡§ (0, 2.8)	<0.001†
	Control	3.4 (1.9, 5.3)	1.7 (0.4, 2.4)	3.8 (2.3, 4.3)	2.9 (2.0, 3.3)	1.5 (0.7, 3.0)	0.10†
	Mann-Whitney *P*	0.47	0.02	<0.001	0.20	0.69	
2	TE	2.0‡ (1.2, 2.3)	2.6‡ (1.7, 2.8)	0‡ (0, 0.7)	2.7‡ (0.7, 4.0)	1.3‡ (0, 3.6)	0.05†
	Control	1.8 (0.8, 3.1) [2.1 ± 1.6]	1.4 (1.2, 2.4) [1.7 ± 0.8]	2.4 (1.1, 2.7) [2.0 ± 0.9]	3.4 (1.7, 5.0) [3.4 ± 2.3]	2.3 (1.0, 3.0) [1.7 ± 1.6]	0.50
	Mann-Whitney *P*	0.89	0.31	0.003	0.70	0.9	
3	TE	0.3 (0, 0.4) [0.5 ± 0.9]‡	5.9 (1.7, 7.8) [5.0 ± 3.0]§	3.4 (1.1, 5.9) [4.0 ± 3.4]‡§	4.7 (2.2, 7.5) [4.8 ± 3.6]‡§	2.3 (1.2, 4.6) [3.0 ± 2.4]‡§	0.02
	Control	0.7 (0.6, 1.0)	0.1 (0, 0.4)	0 (0, 1.0)	0 (0, 0.4)	0.2 (0, 0.9)	0.20†
	Mann-Whitney *P*	0.04	0.002	0.003	0.03	0.04	

Data are the nerve density ($\times 10^5$ μm/mm^3) n = 24, 12, 24, 7, and 12, for each respective time point from before surgery to 12 months after surgery.

* Median (interquartile range: Q25, Q75). Number of combined (surgical and control) corneas at the study time points.

† Kruskal-Wallis one-way ANOVA on ranks was used when data did not satisfy normality and equal variance criteria. When the criteria were met, one-way ANOVA was used [mean ± SD].

‡,§ Where ANOVA indicated significance, median or mean values with the same symbol in each row were not significantly different from each other (Dunn method for ranks or Holm-Sidak method for means).

TABLE 2. Number of Nerve Fiber Bundles per Central Corneal Scan*

Depth Zone	Cornea	Preoperative	Months after Surgery 2	6	10	12	ANOVA *P*†
1	TE	12.5‡ (8.0, 17.0)	0§ (0, 0)	0§ (0, 0)	0‡§ (0, 4.5)	2.0‡§ (0, 7.25)	< 0.001†
	Control	10.5 (7.0, 15.0) [11.3 ± 6.5]	6.0 (2.0, 9.0) [5.8 ± 4.1]	12.0 (5.5, 13.5) [10.6 ± 5.6]	8.0 (5.0, 11.0) [8.0 ± 4.0]	4.0 (2.3, 9.0) [5.4 ± 4.7]	0.15
	Mann-Whitney *P*	0.67	0.009	< 0.001	0.20	0.42	
2	TE	6.0 (3.5, 7.5) [6.3 ± 4.0]	8.5 (6.0, 13.0) [9.3 ± 6.8]	0 (0, 3.2) [1.7 ± 3.2]	12.0 (3.0, 15.8) [9.7 ± 8.7]	3.0 (0, 13.0) [6.6 ± 8.4]	0.07
	Control	7.0 (2.0, 11.5)	5.5 (4.0, 10.0)	6.0 (3.8, 8.8)	14.0 (6.5, 20.0)	8.0 (0.5, 11.5)	0.69†
	Mann-Whitney *P*	0.80	0.39	0.003	0.70	0.90	
3	TE	1.0 (0, 1.3) [1.9 ± 3.5]‡	21.5 (7.0, 24.0) [19.2 ± 12.6]§	13.0 (5.3, 22.3) [15.6 ± 11.9]‡§	17.5 (8.0, 31.5) [19.8 ± 16.8]‡§	8.0 (4.5, 15.0) [9.9 ± 7.4]‡§	0.01
	Control	2.0 (1.8, 3.0)	0.5 (0, 1.0)	0 (0, 3.5)	0 (0, 1.0)	1.0 (0, 2.0)	0.21†
	Mann-Whitney *P*	0.08	0.002	0.001	0.03	0.04	

Data and footnote symbols are as described in Table 1.

whereas in surgical corneas, the nerves were significantly reduced relative to control eyes at 6 months, recovering to control levels at 10 to 12 months. In zone 3, the number and density of nerves remained constant over time in control eyes, while in surgical corneas the nerves were significantly increased in number and density relative to control eyes at all postoperative times.

The number of nerve fiber branches observed within the central cornea correlated strongly with the number of nerves observed ($r = 0.89$ and 0.86 in tissue-engineered and control corneas, respectively), with 57% of all nerve images containing at least one branch. In control corneas, nerve branches were present in similar numbers in zones 1 and 2, whereas they were rare in zone 3 (Table 3). In a manner similar to the trend exhibited by the number and density of nerves, nerve branches in the tissue-engineered corneas were sparse in zone 1, comparable to control corneas in zone 2 (except for a decline at 6 months), and elevated in number relative to control corneas in zone 3.

Nerve fiber bundle diameter in nonsurgical control corneas increased with increasing depth, with a median diameter of 2.3, 2.9, and 6.3 μm in zones 1, 2, and 3, respectively (Fig. 1). The difference in diameter with depth zone in control corneas was significant (Kruskal-Wallis; $P < 0.001$). Median nerve diameter in tissue-engineered corneas was 2.3, 2.3, and 1.7 μm in zones 1, 2, and 3, respectively, and did not vary significantly with depth zone (Kruskal-Wallis $P > 0.05$). From 6 months to 1 year after surgery, the median nerve diameter in zone 3 of tissue-engineered corneas remained significantly lower than in the control corneas (Mann-Whitney $P < 0.05$), whereas the

TABLE 3. Number of Nerve Fiber Branches per Central Corneal Scan*

Depth Zone	Cornea	Preoperative	Months after Surgery 2	6	10	12	ANOVA *P*†
1	TE	5.0‡ (1.5, 6.0)	0‡§ (0, 0.5)	0§ (0, 0)	0‡§ (0, 2.3)	1.5‡§ (0.5, 2.5)	< 0.001†
	Control	4.5 (1.5, 5.5) [4.1 ± 3.1]	1.0 (1.0, 1.5) [1.3 ± 0.5]	4.0 (2.0, 5.0) [3.8 ± 2.4]	3.0 (1.5, 3.8) [2.7 ± 1.5]	0.5 (0, 4.0) [2.0 ± 3.4]	0.31
	Mann-Whitney *P*	0.91	0.06	<0.001	0.2	0.69	
2	TE	3.0‡ (1.5, 4.0)	2.5‡ (2.0, 5.0)	0‡ (0, 0.5)	2.0‡ (0.5, 3.5)	0‡ (0, 1.0)	0.02†
	Control	0 (0, 0.5) [0.8 ± 1.8]‡	2.0 (1.0, 4.0) [2.7 ± 2.1]‡§	3.0 (2.0, 4.5) [3.3 ± 2.1]‡§	9.0 (3.0, 9.8) [6.7 ± 4.9]§	3.0 (0.25, 4.0) [2.4 ± 2.1]‡§	0.02
	Mann-Whitney *P*	0.007	0.7	0.008	0.4	0.26	
3	TE	0.5 (0, 3.0) [1.5 ± 2.4]	6.0 (3.8, 8.3) [6.0 ± 2.6]	3.5 (0, 6.0) [4.3 ± 4.8]	3.0 (3.0, 11.3) [6.7 ± 6.4]	2.5 (1.0, 4.0) [2.5 ± 2.1]	0.29
	Control	1.0 (1.0, 2.0)	0 (0, 0.3)	0 (0, 2.0)	0 (0, 0)	0.5 (0, 1.0)	0.12†
	Mann-Whitney *P*	0.49	0.008	0.08	0.1	0.13	

Data and footnote symbols are as described in Table 1.

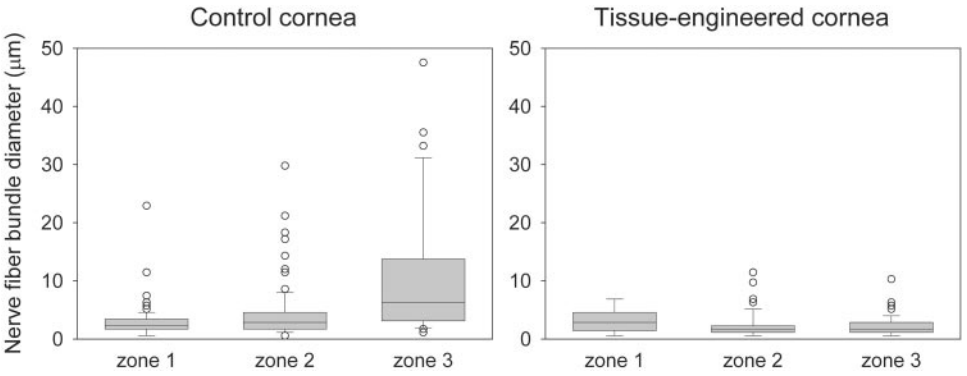

FIGURE 1. Nerve fiber bundle diameter in control corneas (all time points) and postoperative tissue-engineered corneas (all postoperative times). *Box plots* show the distribution of average diameters within an image in each corneal zone, presented as median, interquartile range, and 10th-90th percentiles, with outliers indicated by *open circles*.

number and density of nerves in this region for the same period was greater than in control corneas (Mann-Whitney $P < 0.05$, Tables 1, 2). Morphologically, this was observed as a proliferation of long, thin nerve fiber bundles at the posterior boundary of zone 3 in the tissue-engineered cornea, starting 6 months after surgery (Fig. 2). Light scatter (corneal haze) was observed by confocal microscopy in implanted corneas throughout zones 2 and 3 at the first postoperative examination (2 months), but the scattering within zone 3 had diminished considerably after 6 months, revealing thinner nerves at the transition between zone 3 and the mid stroma. Similarly, reinnervation of zones 2 and 1 was observed as light scatter levels had diminished in zone 2. Zone 1 nerves, however, were not detected until 10 to 12 months after surgery. Regenerated zone 1 nerves in tissue-engineered corneas were observed to have a diameter, density, and general morphology similar to those in control corneas after 1 year, as revealed by in vivo confocal microscopy, and with similar subcellular features, as observed in transmission electron microscope images from histologic sections (Fig. 2).

DISCUSSION

In this study, we have used in vivo confocal microscopy to quantify the pattern of innervation within tissue-engineered and native porcine corneas. In the tissue-engineered corneas, we have shown that nerve regeneration patterns within different collagen-based corneal implants (both with and without chondroitin sulfate) were comparable. Within the native porcine cornea, nerves had a distribution similar to that observed within the human cornea, with the highest density observed closest to the epithelium and decreasing thereafter with increasing depth.[5] Normal human subbasal nerve density in the central cornea has been measured with in vivo confocal microscopy by several investigators (range: 5,867 ± 3,316 to 21,668 ± 1,411 $\mu m/mm^2$, mean ± SD).[5–7,13] The distribution of nerves in relation to depth in the porcine corneas in this study is depicted graphically in Figure 3. In control porcine corneas in this study, the mean subbasal nerve density was 4331 ± 1898 $\mu m/mm^2$ (range: 1,255 to 10,259 $\mu m/mm^2$), determined using the highest single-frame nerve density in zone 1 (26 μm depth of field[22]). The observed porcine subbasal nerve density is within the lower end of the range of reported human nerve density; however, it should be noted that the confocal instrumentation and methodology used varies across the studies. Furthermore, the porcine values may be understated due to nonuniformity in image brightness across the confocal field. Owing to the imaging optics of the confocal microscope (Confoscan 3; Nidek Technologies), image brightness was diminished in the left- and right-hand sides of the image, resulting in an impaired ability to detect the thin, low-contrast subbasal nerves in these areas (covering 20% of the image). The result is a possible underestimate in subbasal nerve density of up to 20%. Stromal nerves, however, generally had a higher contrast relative to the background and were wider in diameter compared with subbasal nerves, and were therefore more easily detected over the complete image area. The observed mean single-image anterior stromal nerve density in control corneas in this study (from zones 2 and 3) was $1.27 \pm 0.57 \times 10^5$ $\mu m/mm^3$, using the 26-μm depth of field with the microscope. To place these values in perspective, normal human stromal nerve density was reported by Oliveira-Soto and Efron[5] as $4.23 \pm 2.06 \times 10^5$ $\mu m/mm^3$ in the anterior stroma, $4.60 \pm 2.32 \times 10^5$ $\mu m/mm^3$ in the anterior–mid stroma, and $3.69 \pm 1.04 \times 10^5$ $\mu m/mm^3$ in the mid stroma, where a 10-μm image depth of field was used.[5] Anterior stromal nerve density in normal human corneas as reported by Calvillo et al.[13] was an order of magnitude below densities found in this study and those reported by Oliveira-Soto and Efron[5]; however, this discrepancy may in part be a result of decreased image brightness and contrast with the tandem scanning system used by Calvillo et al.[13] as noted by McLaren et al.[22] In both our study and that of Oliveira-Soto and Efron,[5] slit-scanning confocal microscopes were used, the method of density determination was the same, and the same microscope objective lens was used. Stromal nerve density in the central porcine cornea, as reported in our study, therefore appears to be lower than the normal human values measured using similar instrumentation. The extent to which these lower densities represent species-dependent or age-dependent differences (pigs in this study were 6 to 18 months of age), however, remains unclear.

Nerve fiber diameter in human corneas is known to increase with increasing corneal depth as thick nerve trunks in the mid stroma branch into successively thinner nerves as they progress upward to innervate the more anterior corneal regions.[5] In an in vivo confocal microscopy study of human corneal nerves, average nerve diameter in the subbasal, anterior, and midstroma was reported as 2.9, 3.7, and 6.3 μm, respectively,[5] similar to diameters measured in porcine control corneas in zones 1, 2, and 3, respectively (see the Results section). Also similar to results obtained in human corneas,[5] the incidence of branching nerves in porcine control corneas decreased with increasing corneal depth, generally after the distribution of nerve density with depth.

The first nerves observed in the center of the tissue-engineered cornea were probably present much earlier, although our study protocol did not permit examination before 2 months after surgery. In zone 3, an increased nerve density relative to control corneas and an absence of thick nerve fiber trunks (diameter, >10 μm) both persisted to 1 year, although it is unclear whether this abnormality in the central cornea would continue in the longer term or have any physiological

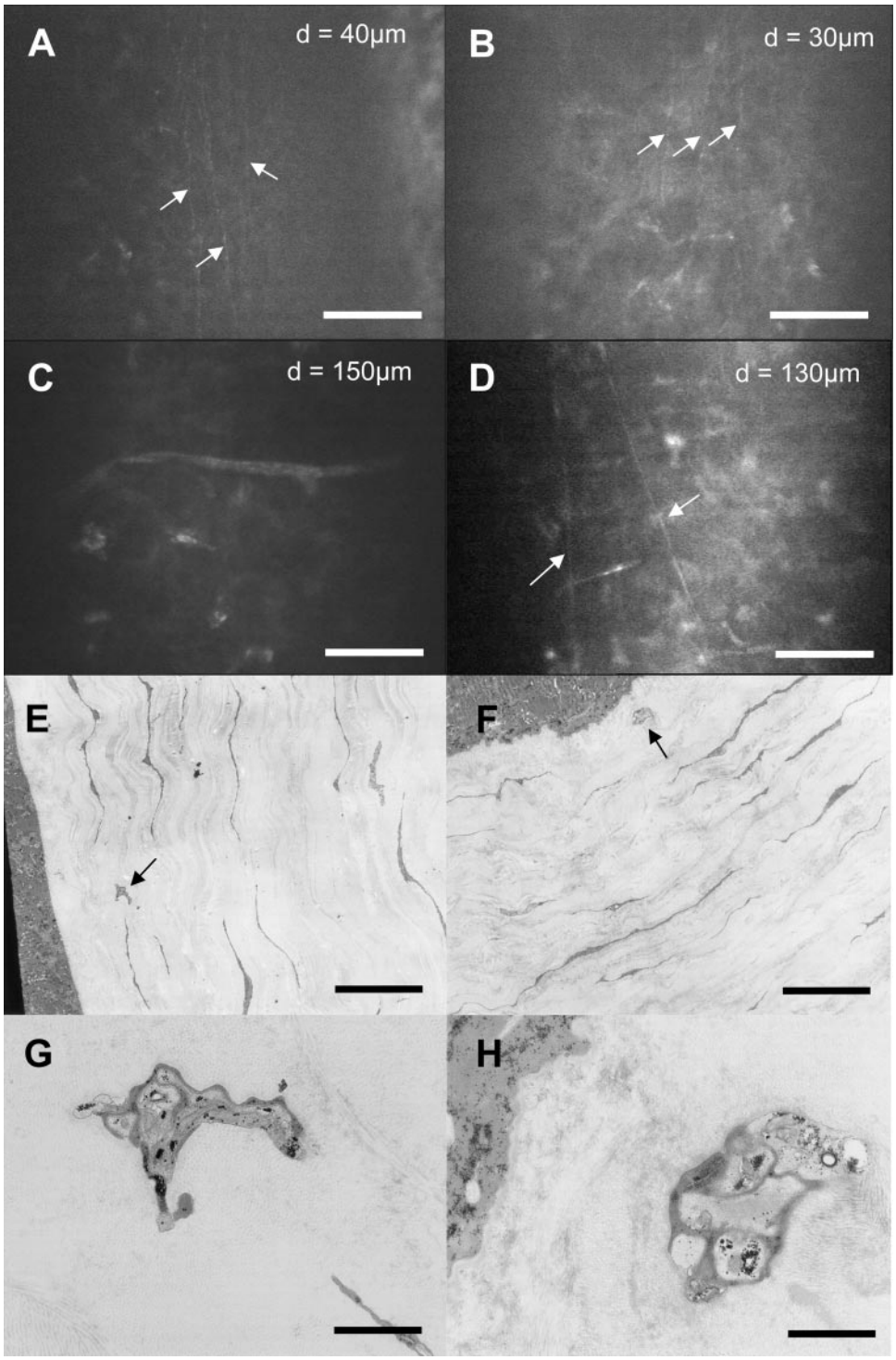

FIGURE 2. Images of nerves within control and tissue-engineered corneas. (**A**) Parallel subbasal nerve fiber bundles with beads in a preoperative control, and (**B**) parallel subbasal nerve fiber bundles within a tissue-engineered cornea (no chondroitin sulfate) 1 year after surgery, with remnants of anterior corneal haze visible in the background. (**C**) Typical nerve fiber in zone 3 of a control cornea at 6 months, and (**D**) thinner regenerated zone 3 nerve fibers in the tissue-engineered cornea of the same animal at 6 months with background corneal haze visible. Transmission electron micrograph cross-sections from control (**E**) and tissue-engineered (**F**) cornea subepithelial regions from the same pig 1 year after surgery. *Black arrows*: subbasal nerve fiber bundles in magnified views (control: **G**; tissue-engineered cornea: **H**), indicating similar cellular and subcellular features. Bar: (**A–D**) 100 μm; (**E**, **F**) 10 μm; (**G**, **H**) 2 μm.

consequences. An absence of nerve trunks within the central corneal stroma suggests that initial reinnervation may have occurred initially in the periphery, followed by nerve branching and growth in a predominantly lateral direction toward the central cornea.

Strong light scatter (or corneal haze) within the implant was detected after surgery by in vivo confocal microscopy and prevented visualization of nerves until the haze had substantially subsided. Although the strong light scatter may have obscured nerve presence, the top boundary of the haze was located within zone 2, leaving zone 1 unaffected. Moreover, within the anterior haze a cavity-like morphology with large transparent voids[23] was observed; however, no nerves were detected within these transparent voids until after the haze had subsided. Only after the haze had diminished substantially were regenerated nerves apparent, first in zone 3, next in zone 2, and finally in zone 1. Although the haze observed was similar in morphology to the scars associated with corneal wound repair after refractive surgery[23,24] and corneal transplantation,[18,25] the reason for the confinement of the haze to a specific depth layer within the central tissue-engineered cornea (spanning a depth of approxi-

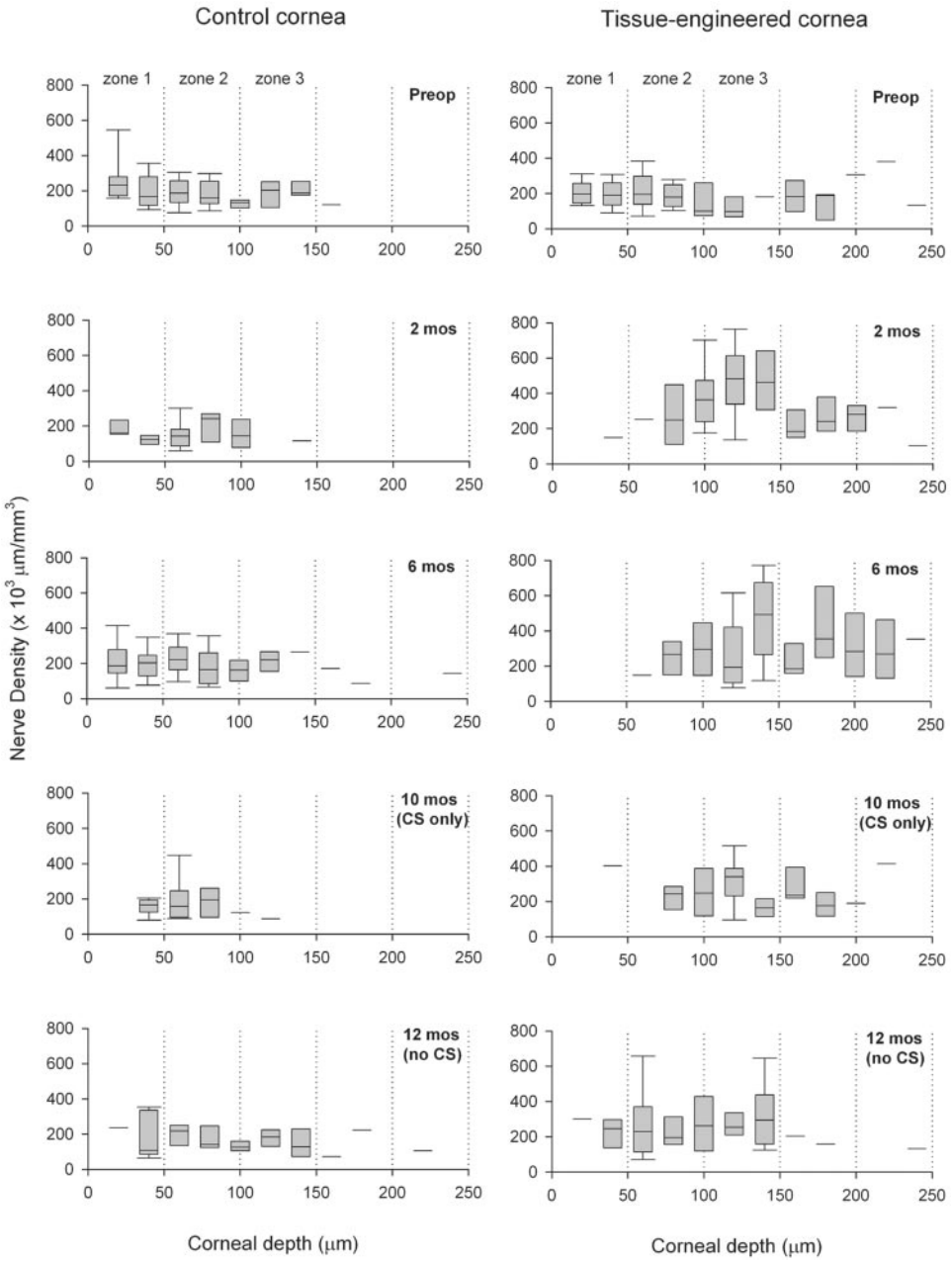

FIGURE 3. Nerve density in control and tissue-engineered corneas. *Box plots* indicate nerve density averaged over two adjacent microscope image frames, presented as median, interquartile range, and 10th-90th percentiles. Where nerve presence was sparse (deeper stroma and regenerating subbasal nerves), median nerve density is shown instead of the box plot. The approximate boundaries of the three corneal depth zones used for analysis are indicated. At 10 months, only animals with chondroitin sulfate tissue-engineered corneas were examined (7 corneas), whereas 12-month data are only from animals without chondroitin sulfate corneas (12 corneas).

mately 100 μm posterior to the basal epithelium) remains unclear.

Remarkably, subbasal nerves within zone 1 regenerated in the tissue-engineered cornea 10 to 12 months after surgery. By comparison, recovery of subbasal nerves in humans has occurred only 2 years after penetrating keratoplasty[18] and 3 to 5 years after refractive surgery.[24,26] Although the protocol of the present study precluded the correlation of corneal sensitivity measurements by esthesiometry with the in vivo confocal microscopy results, subbasal innervation of the tissue-engineered cornea indicates a likely return of corneal touch sensitivity.

In a qualitative in vivo confocal microscopy study of reinnervation after penetrating keratoplasty,[18] the first central corneal nerves appeared in the anterior to mid stroma after 7 months, with an abnormally twisted morphology. Although in the tissue-engineered cornea the first central corneal nerves appeared earlier, implants in this study underwent a milder surgical trauma in lamellar keratoplasty compared with the penetrating keratoplasty procedure.

Finally, no significant trend specific to nerve branch presence could be detected in this study. This finding may either indicate that nerve sprouting and branching occurs equally well within the native and the tissue-engineered cornea or that a larger number of total nerve branches is needed to detect specific branching effects (564 branches versus 1835 nerves were observed among all corneas in this study).

In summary, we revealed the quantitative pattern of innervation within tissue-engineered corneal substitutes implanted in live porcine hosts over a 1-year period. After 1 year, the number and density of nerves in the central region of the tissue-engineered cornea was significantly greater than or not significantly different from levels in nonsurgical control corneas in the three corneal depth zones examined. The structure of the most anterior nerves within the tissue-engineered corneas closely resembled nerves within nonsurgical control cor-

neas as determined by both in vivo confocal microscopy and transmission electron microscopy. These findings indicate the suitability of the cross-linked, collagen-based, tissue-engineered cornea for neural regeneration, and provide an objective basis for assessing the long-term neural status of tissue-engineered corneas in future animal and human studies.

Acknowledgments

The authors thank Donna Bueckert, Cecilia Becerril, and Lea Muzakare for excellent technical support; Yasuhiro Kato (TDC Eye Bank, Chiba, Japan) and Minoru Fukuda (Laboratory of electron microscopy, Kyorin University School of Medicine, Tokyo, Japan) for electron microscopy support; Yuwen Liu and Fengfu Li for TE cornea fabrication; and Marilyn Keaney, MD, and her team (University of Ottawa Animal Care and Veterinary Services) for contributions to our research.

References

1. Whitcher JP, Srinivasan M, Upadhyay MP. Corneal blindness: a global perspective. *Bull World Health Organ*. 2001;79:214–221.
2. Li F, Carlsson DJ, Lohmann CP, et al. Cellular and nerve regeneration within a biosynthetic extracellular matrix for corneal transplantation. *Proc Natl Acad Sci USA*. 2003;100:15346–15351.
3. Liu Y, Gan L, Carlsson DJ, et al. A simple, cross-linked collagen tissue substitute for corneal implantation. *Invest Ophthalmol Vis Sci*. 2006;47:1869–1875.
4. Krachmer JH, Mannis MJ, Holland EJ, eds. *Cornea.* 2nd ed. St. Louis, MO: Elsevier Mosby; 2005;21.
5. Oliveira-Soto L, Efron N. Morphology of corneal nerves using confocal microscopy. *Cornea*. 2001;20:374–384.
6. Grupcheva CN, Wong T, Riley AF, McGhee CNJ. Assessing the sub-basal nerve plexus of the living healthy human cornea by *in vivo* confocal microscopy. *Clin Exp Ophthalmol*. 2002;30:187–190.
7. Patel DV, McGhee CNJ. Mapping of the normal human corneal sub-basal nerve plexus by in vivo laser scanning confocal microscopy. *Invest Ophthalmol Vis Sci*. 2005;46:4485–4488.
8. Tuominen ISJ, Konttinen YT, Vesaluoma MH, Moilanen JAO, Helintö M, Tervo TMT. Corneal innervation and morphology in primary Sjögren's syndrome. *Invest Ophthalmol Vis Sci*. 2003;44:2545–2549.
9. Mannion LS, Tromans C, O'Donnell C. An evaluation of corneal nerve morphology and function in moderate keratoconus. *Cont Lens Ant Eye*. 2005;28:185–192.
10. Hossain P, Sachdev A, Malik RA. Early detection of diabetic peripheral neuropathy with corneal confocal microscopy. *Lancet*. 2005;366:1340–1343.
11. Linna TU, Minna HV, Pérez-Santonja JJ, Petroll WM, Alió JL, Tervo TMT. Effect of myopic LASIK on corneal sensitivity and morphology of subbasal nerves. *Invest Ophthalmol Vis Sci*. 2000;41:393–397.
12. Erie JC, Patel SV, Bourne WM. Aberrant corneal nerve regeneration after PRK. *Cornea*. 2003;22:684–686.
13. Calvillo MP, McLaren JW, Hodge DO, Bourne WM. Corneal reinnervation after LASIK: prospective 3-year longitudinal study. *Invest Ophthalmol Vis Sci*. 2004;45:3991–3996.
14. Bragheeth MA, Dua HS. Corneal sensation after myopic and hyperopic LASIK: clinical and confocal microscopic study. *Br J Ophthalmol*. 2005;89:580–585.
15. Tervo T, Vannas A, Tervo K, Holden BA. Histochemical evidence of limited reinnervation of human corneal grafts. *Acta Ophthalmol*. 1985;63:207–214.
16. Rao GN, John T, Ishida N, Aquavella JV. Recovery of corneal sensitivity in grafts following penetrating keratoplasty. *Ophthalmology*. 1985;92:1408–1411.
17. Bohm A, Kohlhaas M, Kliefoth U, et al. Corneal reinnervation after lamellar keratoplasty in comparison with epikeratophakia and photorefractive keratectomy. *Ophthalmologe*. 1994;91:632–637.
18. Richter A, Slowik C, Somodi S, Vick HP, Guthoff R. Corneal reinnervation following penetrating keratoplasty: correlation of esthesiometry and confocal microscopy. *Ger J Ophthalmol*. 1996;5:513–517.
19. Erskine L, McCaig CD. Integrated interactions between chondroitin sulphate proteoglycans and weak dc electric fields regulate nerve growth cone guidance in vitro. *J Cell Sci*. 1997;110:1957–1965.
20. Abramoff MD, Magelhaes PJ, Ram SJ. Image processing with Image. *J Biophoton Int*. 2004;11:36–42.
21. Meijering E, Jacob M, Sarria J-CF, Steiner P, Hirling H, Unser M. Design and validation of a tool for neurite tracing and analysis in fluorescence microscopy images. *Cytometry*. 2004;58:167–176.
22. McLaren JW, Nau CB, Kitzmann AS, Bourne WM. Keratocyte density: comparison of two confocal microscopes. *Eye Cont Lens*. 2005;31:28–33.
23. Møller-Pedersen T, Cavanagh HD, Petroll WM, Jester JV. Stromal wound healing explains refractive instability and haze development after photorefractive keratectomy: a 1-year confocal microscopic study. *Ophthalmology*. 2000;107:1235–1245.
24. Tervo T, Moilanen J. In vivo confocal microscopy for evaluation of wound healing following corneal refractive surgery. *Prog Retin Eye Res*. 2003;22:339–358.
25. Bourne WM. Cellular changes in transplanted human corneas. *Cornea*. 2001;20:560–569.
26. Erie JC, McLaren JW, Hodge DO, Bourne WM. Recovery of corneal subbasal nerve density after PRK and LASIK. *Am J Ophthalmol*. 2005;140:1059–1064.